Effects of UD and twill reinforcements in hybrid sheet molding compound laminates

RAIMONDI Luca[1,a *], BRUGO Tommaso Maria[1,b], ZUCCHELLI Andrea[1,c] and DONATI Lorenzo[1,d]

[1]Viale Risorgimento 2, Bologna, Italy

[a]luca.raimondi@unibo.it, [b]tommasomaria.brugo@unibo.it, [c]a.zucchelli@unibo.it, [d]l.donati@unibo.it

Keywords: Carbon Fiber, Compression Molding, Sheet Molding Compound, Hybrid Composites

Abstract. This work proposes a novel manufacturing solution to locally reinforce a Sheet Molding Compound (SMC) with continuous fiber prepreg in a single-step compression molding operation. An adapted SMC process allowing for the manufacturing of continuous carbon fiber-reinforced SMC was successfully implemented, and a layer of fabric was added to mitigate the waviness induced during processing. Plates with different stacking sequences were manufactured and used for mechanical characterization to understand the effect of hybridization over tensile and flexural properties. It emerges that hybridization led to a 137% increase in tensile strength and up to 147% rise in flexural modulus compared to the standard SMC baseline. Additionally, the hybridization process helped reduce the variability in elastic and strength properties.

Introduction

Driven by the need to reduce operating costs and increase performance and safety, the transport industry is looking for advanced, high-specific strength materials to meet cost, quality, and volume targets. Discontinued fiber-reinforced composite materials are appreciated for their high processability, high stiffness [1], notch insensitivity [2], and ability to withstand harsh environmental conditions [3]. However, they exhibit relatively low strength due to their limited reinforcement length. Unidirectional and continuous fiber-reinforced composites are highly regarded for their impressive specific stiffness and strength as well as for their capability of energy absorption in the event of a crash [4,5], but have limited design flexibility due to poor formability. The concept of integrating continuous reinforcements with discontinuous fiber reinforced in the form of Sheet Molding Compound (SMC) presents a promising solution to overcome the inherent limitations of both materials. While the concept of blending discontinuous SMC with continuous fibrous reinforcements originated in the 1970s [6,7], to the best of the authors' knowledge, comprehensive studies specifically focused on understanding hybrid SMC materials have been conducted for approximately the past five years. A potential limitation dictated by the technology arises from the opposite need to establish appropriate flow in the short-fiber layers and to limit the mobility of the long-fiber composite layers to prevent misalignment phenomena during molding. Strategies to mitigate these defects include staging the long fiber reinforced prepreg resin before molding [9] or using dual-stage resin systems [8,9]. Although these strategies have proven effective against defect formation, they require prior processing in an oven or to alter the temperature of the tool during forming, which slows down the production time of the manufactured part. The possibility of manufacturing hybrid laminates in a single-step compression molding operation is investigated in this work. An adapted SMC process allowing for the manufacturing of continuous carbon fiber reinforced SMC was successfully implemented, and a layer of fabric was added to mitigate the waviness induced during processing. Plates with different stacking sequences were manufactured and used for mechanical characterization to understand the effect of hybridization over tensile and flexural properties. Before mechanical testing, fiber misalignment of the endless fiber reinforcements was characterized by the Full Field Nodal Method (FFNM) [10] to measure the quality of the produced plates.

Materials and Methods

Materials, plate manufacturing, and sample extraction. In this study, three materials were used: a sheet molding compound (SMC) prepreg, a unidirectional prepreg (UD), and a twill (TW) prepreg. The SMC used was HexMC/C/2000/M77, supplied by Hexcel (Duxford, U.K.). This SMC comprises randomly oriented 25 mm long carbon fiber strands impregnated with M77 epoxy resin. M77 is a fast-curing epoxy specifically designed for compression molding. The UD used was Toray prepreg P 384_S, supplied by Torayca (Tokyo, Japan). It is made of high-strength carbon fibers and impregnated with 40% #2300 resin, both manufactured by Toray Industries. The TW prepreg used was a 2x2 fabric SC160/RC200P supplied by Gurit (Volpiano, IT). This TW is made of standard modulus carbon fibers manufactured by Toray Industries and impregnated with a 40% GURIT SC160 epoxy resin. Different charge configurations for misalignment analysis and mechanical characterization of the three materials and their combination were considered. A mold coverage of 100% was adopted to manufacture the continuous fiber plates to prevent material flow during the process. The prepreg was cut into 320 [mm] x 240 [mm] rectangular preforms to manufacture the SMC plaques, achieving 80% tool coverage and allowing a one-dimensional flow during compression molding. UD and TW patches were first laminated with 100% areal coverage to produce the continuous reinforcement. The protocol described in [10,11] was adopted to measure the process induced waviness of external plies. An uniform 35 [mm] x 35 [mm] grid was drawn on the surface of the wet prepreg by using a 3 mm wide Berner paint marker. Images of gridded uncured plates were acquired into a Kyocera TASKalfa 3501i Multifunction Laser Printer at a resolution of 600 × 600 dpi and stored for subsequent processing. Afterwards, the charge was completed by stacking an 80% areal coverage SMC laminate and then compression molded in a one-step compression molding operation as schematically represented in Figure 1.

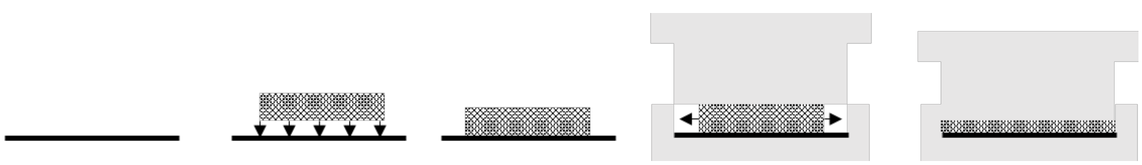

Figure 1: Compression molding of hybrid plates.

An overview of the staking sequence and designation used for each plaque's charge is provided in Table 1. For example, UD2/100%/SMC2/80% consists of two plies of UD having a tool coverage area of 100% stacked onto two plies of SMC with an areal coverage of 80%. The compression molding was performed using a specialized tool measuring 320 [mm] x 320 [mm], designed to produce plates with arbitrary thicknesses. The tool was installed in a downstroke AEM3 press, and its temperature was maintained at a constant 130°C, which was verified by two thermocouples. Once cured, the plaques were extracted, cooled in free air until they reached room temperature, and scanned using at a resolution of 600 × 600 dpi. The size of the plaques allows for the extraction of at least 5 samples for each mechanical testing configuration. The specimens were cut using abrasive water jet cutting and stored at room temperature with medium relative humidity for seven days before testing.

Materials Research Proceedings 41 (2024) 523-529 https://doi.org/10.21741/9781644903131-58

Table 1: Plaque stacking and molding details for different material combinations.

Study #. Plaque #	Designation	# UD plies	# TW plies	# SMC plies	Charge coverage
1.1	SMC3/80%			3	80%
1.2	SMC8/80%			8	80%
2.1	UD2/100%	2			100%
2.2	UD14/100%	14			100%
3.1	TW6/100%		6		100%
3.2	TW10/100%		10		100%
4.1	UD2/100%/TW1/100%/SMC2/80%	2	1	2	100%/100%/80%

In order to avoid any potential damage to the outer layers of continuous carbon fiber-reinforced material during testing, end tabs were used on tensile samples. To prepare for adhesive bonding, both sides of the samples were conditioned with 180-grit sandpaper and cleaned with isopropyl alcohol. Tapered SMC end tabs, which were 2.5 [mm] thick, 50 [mm] long, and 25 [mm] wide, were then bonded onto the specimens.

Mechanical testing. The specimens for tensile testing were designed according to the standard test method ASTM D3039/D3039M and featured a length of 250 [mm] and a width of 25 [mm]. Tests were conducted at a constant cross-head rate of 2.5 [mm/min] using a servo-hydraulic INSTRON 8033 universal testing machine equipped with a 250 [kN] load cell under displacement-controlled conditions. The sample's surfaces were monitored by the two cameras of a commercial 3D Digital Image Correlation (DIC) system (Q-400, Dantec Dynamics, Skovlunde, Denmark) equipped with 17-mm lenses (Xenoplan, Schneider-Kreuznach, Bad Kreuznach, Germany) to allow for reliable measurement of surface deformation as suggested by [12]. The specimen surface was coated with a water-based paint (black matt, Chreon, Lechler, Como, Italy). For the speckle dots, white paint was used (white matt, Chreon, Lechler). The paints were deposited on the specimens by means of an airbrush spray gun (AZ3 HTE 2, Antes Iwata, Torino, Italy) with a nozzle of 1.8 [mm], a round jet, and a spray distance of about 300 [mm]. The Istra-4D software from Dantec Dynamics was used to analyze images, determine displacements, and strain distributions. The facet size was set to 25 pixels, and the facet overlap to 9 pixels. A local regression displacement smoothing filter of 25 x 25 facets was applied to balance accuracy and spatial resolution [10]. The specimens for flexural testing were designed according to the standard test method ASTM D790-17. To minimize through-thickness shear effects, a span-to-thickness ratio greater than 16:1 was adopted. Specimens were loaded to failure at a constant cross-head rate of 1 [mm/min] using a 2 [kN] load cell.

Result and discussion

Results from the misalignment analysis by FFNM on representative plates is given in Figure 2. Due to the intense processing pressure, both UD2/100% and UD14/100% plaques exhibited an in-plane fiber waviness in the range [-5° 5°] (Figure 2a), demonstrating that this material was able to flow even at 100% areal coverage. Apparent in-plane waviness was much less pronounced in TW6/100% and TW10/100% plaques, being consistently in the range of [0° 2°] as reported in Figure 2b. In-plane fiber waviness of the outer layer of UD2/100%/TW1/100%/SMC2/80% hybrid plaques was consistently in the range of [-3° 2°], demonstrating the effectiveness of TW fabric in preventing lateral motion of UD fibers during processing.

Materials Research Proceedings 41 (2024) 523-529 https://doi.org/10.21741/9781644903131-58

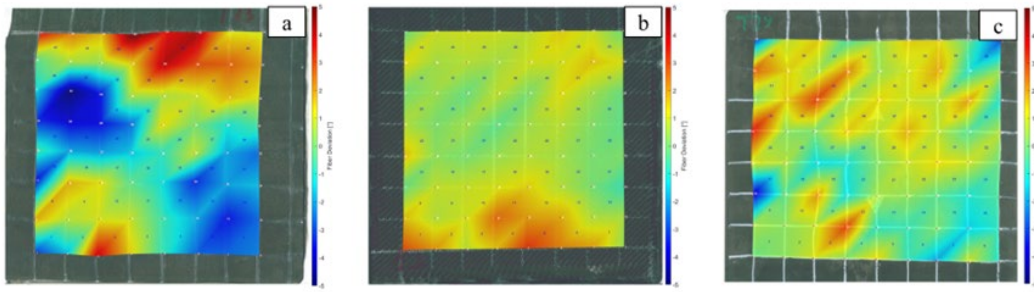

Figure 2: Fiber misalignment analysis of manufactured plates measured by FFNM technique. a) UD2/100% b) TW6/100% c) UD2/100%/TW1/100%/SMC2/80%

Results from mechanical tests are summarized in Figure 3. Good repeatability was found for the elastic and tensile properties of discontinuous laminates with hybridization. The coefficient of variations (CV) was below 10% for the elastic modulus and below 5% for the ultimate tensile strength of UD and TW samples. However, the ultimate tensile strength of SMC specimens had a high scatter, with a CV of nearly 20%. The benefits of hybridization in stabilizing both elastic and ultimate tensile strength were confirmed by the low CV value of 6% for UD2/100%/TW1/100%/SMC2/80% samples. Comparable results were obtained in flexural tests. CV values for both UD and TW were below 5% for both flexural modulus and ultimate stress. On the other hand, the SMC samples demonstrated significant variability with a CV of 38% in modulus. The repeatability of results for hybrid UD2/100%/TW1/100%/SMC2/80% samples depended on the loading conditions of the continuous reinforcement.

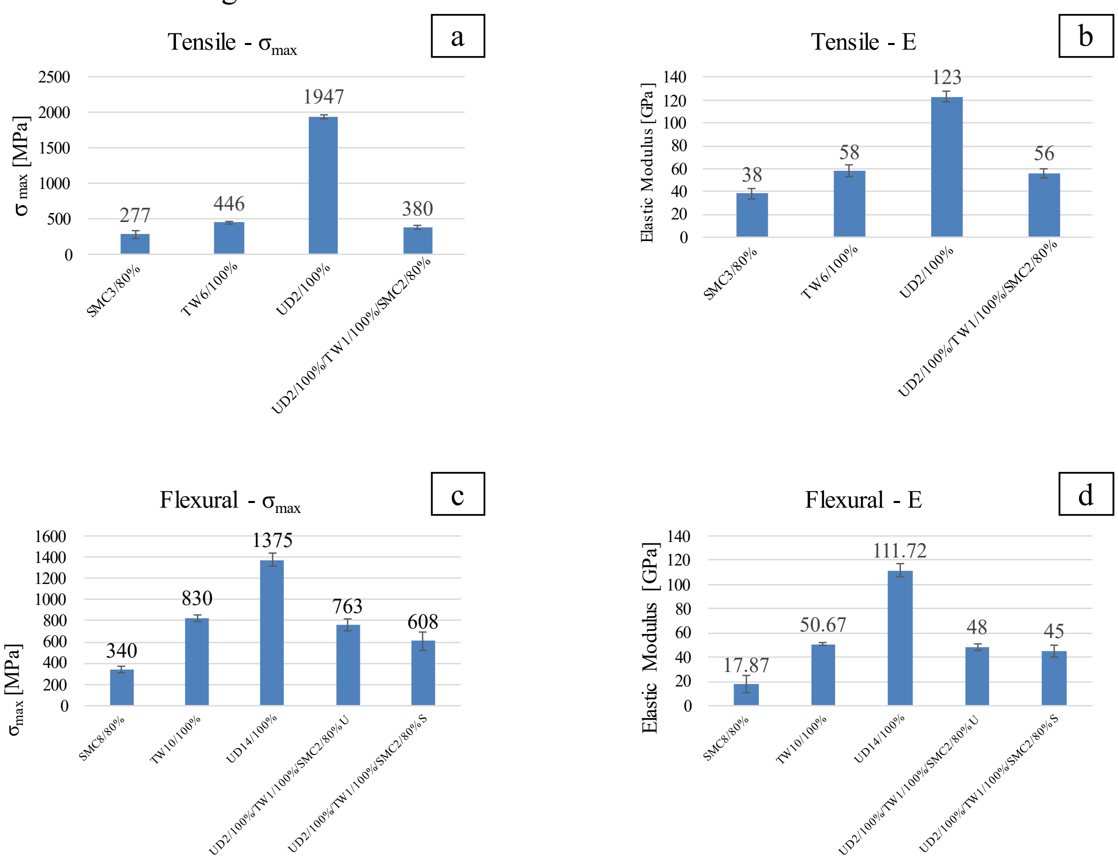

Figure 3: Mechanical test results. a) tensile strength; b) tensile modulus; c) flexural strength d) flexural modulus

In the specimens where the long-fiber reinforcement was placed in tension during the test, the CVs of flexural modulus and tensile strength were found to be 7% and 5%, respectively. On the other hand, in specimens where the long-fiber reinforcement was placed in compression, the CVs of flexural modulus and tensile strength increased to 15% and 10%, respectively. Both tensile and flexural modulus of hybrid laminate was comparable to the ones of TW (Figure 3b, Figure 3c) although their resistance was slightly lower. A significative improvement in bending strength can be achieved by positioning the continuous reinforcement in traction, which contributes in increase the resistance by an additional 20% (Figure 3c). Representative stress-strain curves are shown in Figure 3. UD sets the upper bound for stiffness and strength among base laminates, while SMC sets the lower bound. The typical behavior of the stress-strain curve in tensile for all laminate is mostly linear except for the last 10% of the strain for UD2/100% material where the curves usually tend to be non-linear (Figure 4a) due to progressive failure of the material. In a previous study by the authors [10], it was observed that the initial macroscopic failure of UD2/100% specimens occurred in the areas where the maximum absolute value of fiber waviness was detected. Stress-strain curves for SMC3/80%, TW6/100%, and UD2/100%/TW1/100%/SMC2/80% samples in tensile tests exhibited consistent linear behavior until failure. Stress strain curves from flexural test highlight the different failure mechanisms of the materials used. Both UD14/100% and TW10/100% samples exhibited a linear region followed by a sudden load drop before abrupt failure. The strain field resulting from flexural tests of SMC8/80% samples was qualitatively spoken homogeneous in the beginning of loading. Afterwards a number of load-drops followed by load recovery was consistently observed across all samples, indicating the progressive damage of the material. It can be argued that these phenomena are strictly related to the heterogeneous microstructure of the SMC material, capable to provide a stress redistribution after onset of damage such as fiber debonding or cracking of the matrix [13].

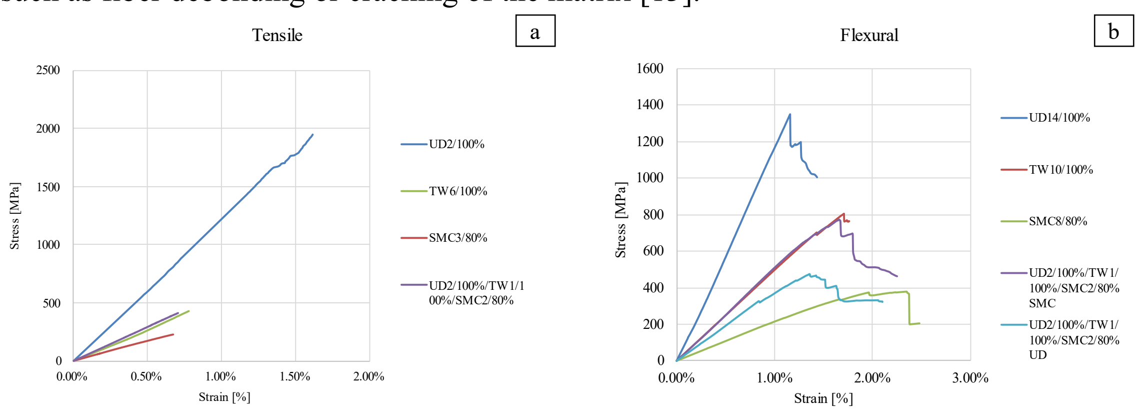

Figure 4: Representative stress-strain curves from mechanical characterization. a) tensile b) flexural

When short fibers are loaded in tension, these phenomena are observable also at intermediate loads on UD2/100%/TW1/100%/SMC2/80% samples as visible in Figure 4b. At higher loads, the hybrid laminate gradually fails, with several consecutive load drops preceding the final failure of the sample. When short fibers are loaded in compression, no load drop is visible on UD2/100%/TW1/100%/SMC2/80% samples. Up to the point of first failure, the stress-strain curve for this configuration overlaps with the TW samples. However, due to the inherent capacity of SMC to internally redistribute stresses, this configuration provides additional load-bearing capacity as visible by the largest deformation at break shown in Figure 4b. The DIC analysis provided a great insight in understanding the failure mechanisms of hybrid UD2/100%/TW1/100%/SMC2/80% samples during loading. On the SMC side of the specimen, the strain distribution was non uniform. Localized high strain-concentrated areas appeared at a fraction of the ultimate load (Figure 5a), probably due to the interaction between bundle ends and transverse fibers [14]. As the load increases, fractures occur locally, leading to a redistribution of strain (Figure 5b) without noticeably affecting the stress-strain response of the sample. When strain concentration appears at the interface with the SMC and the endless fiber reinforcement, strain a wider area is affected (Figure 5c). With increasing load, damage on continuous fibers increases (Figure 5d) dealing with the failure of the continuous fiber reinforcement.

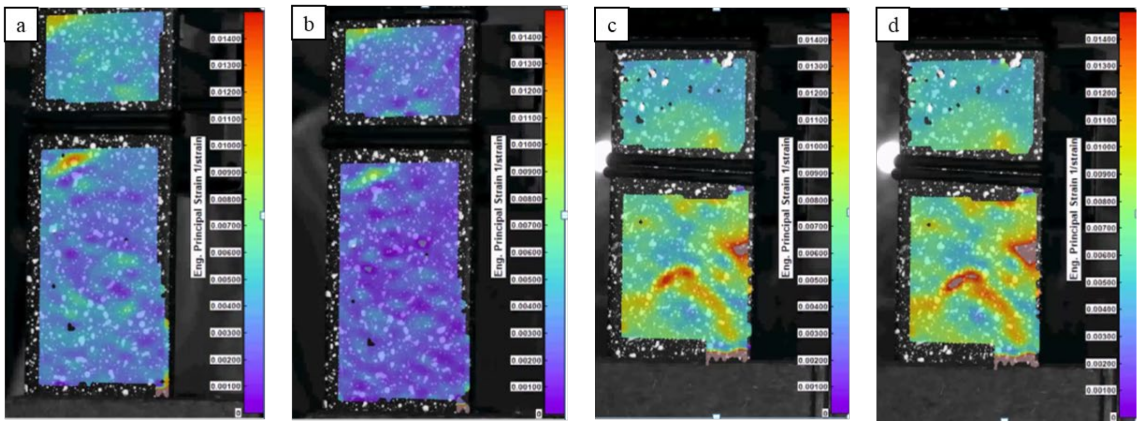

Figure 5: Strain distribution on the surface of a UD2/100%/TW1/100%/SMC2/80% samples at different loads. a) SMC side at 70% of ultimate load b) SMC side at 90% of ultimate load c) UD side side at 70% of ultimate load d) SMC side at 90% of ultimate load

Conclusions

A viable technological solution for the manufacturing of flat components with hybrid fiber architecture laminates in a single step compression molding operation was proposed in this work by integrating a layer of fabric to mitigate the waviness induced during processing. Specimens were extracted on compression molded plates and successfully tested in tensile and flexure. Main findings are the follow:

- Hybridization led to a 137% increase in tensile strength and up to 147% rise in flexural modulus compared to the standard SMC baseline.
- The standard deviation on tensile strengths and elastic modulus of the hybrid laminate is consistently comparable to that of a long-fiber system.

Future works will investigate the reliability of numerical simulation tools in predicting the quality of compression molded parts with hybrid fiber architectures. Simulations based on state of the art strategies will be used to predict wrinkles and other forming effects which can occur in the continuous reinforcement during molding of complex parts [15]. Interactions between SMC flow and endless fiber reinforcement will be numerically studied by means of direct fiber simulation [16]. The process simulation results will be used for the development of a suitable simulation model for virtual test of individual materials as well as hybrid-architectures.

References

[1] Zulueta K, Arrillaga A, Stelzer PS, Martinez I. An evaluation of the curing characteristics of thermosetting epoxy carbon fiber sheet molding compounds and validation through computer simulations and molding trials. J Appl Polym Sci 2021;138. https://doi.org/10.1002/app.50826

[2] Feraboli P, Peitso E, Cleveland T, Stickler PB, Halpin JC, Feraboli Paolo, Peitso Elof, Cleveland Tyler, Stickler HJC. Notched behavior of prepreg-based discontinuous carbon fiber/epoxy systems. Compos Part A Appl Sci Manuf 2009;40:289–99. https://doi.org/10.1016/j.compositesa.2008.12.012

[3] Laribi MA, TieBi R, Tamboura S, Shirinbayan M, Tcharkhtchi A, Dali H Ben, et al. Sheet Molding Compound Automotive Component Reliability Using a Micromechanical Damage Approach. Appl Compos Mater 2020;27:693–715. https://doi.org/10.1007/s10443-020-09831-5

[4] Falaschetti MP, Rondina F, Maccaferri E, Mazzocchetti L, Donati L, Zucchelli A, et al. Improving the crashworthiness of CFRP structures by rubbery nanofibrous interlayers. Compos Struct 2023;311. https://doi.org/10.1016/j.compstruct.2023.116845

[5] Rondina F, Falaschetti MP, Zavatta N, Donati L. Numerical simulation of the compression crushing energy of carbon fiber-epoxy woven composite structures. Compos Struct 2023;303. https://doi.org/10.1016/j.compstruct.2022.116300

[6] Mallick PK. Effect of fiber misorientation on the tensile strength of compression molded continuous fiber composites. Polym Compos 1986;7:14–8. https://doi.org/10.1002/pc.750070104.

[7] DG Taggart, RB Pipes, RA Blake, JW Gillespie Jr, R Prabhakaran JW. Properties of SMC composites. Cent Compos Mater Univ Delaware 1979.

[8] Trauth A, Weidenmann KA. Continuous-discontinuous sheet moulding compounds – Effect of hybridisation on mechanical material properties. Compos Struct 2018. https://doi.org/10.1016/j.compstruct.2018.05.048

[9] Trauth A, Weidenmann KA, Altenhof W. Puncture properties of a hybrid continuous-discontinuous sheet moulding compound for structural applications. Compos Part B Eng 2019;158:46–54. https://doi.org/10.1016/j.compositesb.2018.09.035

[10] Raimondi L, Brugo TM, Zucchelli A. Fiber misalignment analysis in PCM-UD composite materials by Full Field Nodal Method. Compos Part C Open Access 2021;5. https://doi.org/10.1016/j.jcomc.2021.100151

[11] Corbridge DM, Harper LT, De Focatiis DSA, Warrior NA. Compression moulding of composites with hybrid fibre architectures. Compos Part A Appl Sci Manuf 2017. https://doi.org/10.1016/j.compositesa.2016.12.018

[12] Feraboli P, Peitso E, Cleveland T, Stickler PB. Modulus measurement for prepreg-based discontinuous carbon fiber/epoxy systems. J Compos Mater 2009;43:1947–65. https://doi.org/10.1177/0021998309343028

[13] Visweswaraiah SB, Selezneva M, Lessard L, Hubert P. Mechanical characterisation and modelling of randomly oriented strand architecture and their hybrids – A general review. J Reinf Plast Compos 2018;37:548–80. https://doi.org/10.1177/0731684418754360

[14] Johanson K, Harper LT, Johnson MS, Warrior NA. Heterogeneity of discontinuous carbon fibre composites: Damage initiation captured by Digital Image Correlation. Compos Part A Appl Sci Manuf 2015;68:304–12. https://doi.org/10.1016/j.compositesa.2014.10.014

[15] Boisse P, Akkerman R, Carlone P, Kärger L, Lomov S V., Sherwood JA. Advances in composite forming through 25 years of ESAFORM. Int J Mater Form 2022;15. https://doi.org/10.1007/s12289-022-01682-8

[16] Qian CC, Deshpande A, Jesri M, Groves R, Reynolds N, Kendall K. A comprehensive assessment of commercial process simulation software for compression moulding of sheet moulding compound. ESAFORM 2021 - 24th Int. Conf. Mater. Form., 2021. https://doi.org/10.25518/esaform21.2771